IRFOC induction motor with rotor time constant estimation modelling and simulation

E. Radwan
School of Engineering, University College Sedaya International (UCSI), Taman Connaught, Cheras, Kuala Lumpur, Malaysia

N. Mariun, I. Aris and S.M. Bash
Department of Electrical and Electronics Engineering, Faculty of Engineering, Universiti Putra Malaysia (UPM), Serdang, Malaysia, and

A.H. Yatim
Department of Energy Conversion, Faculty of Electrical Engineering, Universiti Teknologi Malaysia (UTM), Skudai, Johor, Malaysia

Received September 2003
Revised October 2004
Accepted November 2004

Abstract

Purpose – To provide a new and simple inverse rotor time constant identification method which can be used to update an indirect rotor field oriented controlled (IRFOC) induction motor algorithm.

Design/methodology/approach – Two different equations are used to estimate the rotor flux in the stator reference frame. One of the equations is a function of the rotor time constant, rotor angular velocity and the stator currents. The other equation is a function of measured stator currents and voltages. The equation that uses the voltage and the current signals of the stator serves as reference model, however, the other equation works as an adjustable model with respect to the variation of the rotor time constant. Voltage signals used in the reference model equation are obtained from the measured DC bus voltage and the inverter gating signals. The proposed scheme is verified using a MATLAB/SIMULINK model for two different motors and experimentally using a DSP development tool (MCK 243) supplied by Technosoft S.A.

Findings – The proposed estimator was able to successfully track the actual value of the inverse rotor time constant for different load torque and speed operating conditions. Increased oscillations in the estimated inverse rotor time constant appeared at lower speeds (below 10 per cent of rated speed) due to drift in a PI regulator (used at the estimator side), which was tuned under rated operating conditions and using parameters nominal values.

Research limitations/implications – This estimation scheme is limited when near zero speed operation is demanded; otherwise it gives a simple and practical solution. A suggested way out of this, is to provide a self-tuning controller that can automatically adjust even for zero speed operation, or to automatically disconnect the estimator and take the most updated value as long as the operating speed is below a predetermined value.

Originality/value – This paper presented a new inverse rotor time constant estimator for an IRFOC induction motor application and in conjunction rotor flux was estimated without voltage phase sensors.

The authors would like to thank Dr Mohand Ouhrouche (Department of Applied Science, University of Quebec at Chicoutimi, Canada) for many helpful suggestions and valuable comments. The authors would also like to express their deepest appreciation to University Putra Malaysia (UPM) and Dr Shamsul Bahri for supporting this work.

COMPEL: The International Journal for Computation and Mathematics in Electrical and Electronic Engineering
Vol. 24 No. 4, 2005
pp. 1093-1119

0332-1649
DOI 10.1108/03321640510615481

Keywords Inductance, Electric motors, Programming and algorithm theory
Paper type Research paper

1. Introduction

Field oriented control has widely been used to obtain improved control performance of induction motor drives. In general field oriented control can be classified into direct and indirect field orientation control, the main difference being that direct field orientation control is accomplished with help of measurement sensors or estimation of the flux to obtain the rotor flux angle. While indirect field oriented control (IFOC) is accomplished by utilization of feed forward slip command and feedback velocity signal to obtain the decoupling angle. However, the transient performance of both filed orientation is determined primarily by accuracy of the motor parameters used in the field orientation (Shieh *et al.*, 1998).

Since its introduction in the early 1980s the direct rotor field orientation scheme has been regarded as less practical because of the sensors needed for obtaining information about the machine variables. In addition to increasing the total controller cost, these sensors often impose limitations on the machine operating range (Moreira *et al.*, 1992). The absence of field angle sensors, the ease of implementation, and the better overall performance especially at low frequencies has increased the popularity of the IFOC scheme (Ba-razzouk *et al.*, 1999). The major disadvantage of the IFOC scheme is that it is machine parameter dependent since the model of the motor is used for flux estimation. Among the motor parameters the rotor time constant is the parameter that mostly influence IFOC control scheme, since it depends on the temperature, the saturation level and the skin effect (Ba-razzouk *et al.*, 1999; Hren and Jezernik, 1997). Moreover, as the rotor in an induction machine (cage type) is physically isolated and not reachable for measurements most of the time (compared with the stator), it is difficult to obtain a good and accurate initial estimation for that parameter. Various schemes have been proposed for parameter estimation for such a drive over the past two decades, and can be divided into three groups (Hren and Jezernik, 1997):

- Estimation based on injection of a high frequency external perturbation signal,
- Estimation based on an error signal usually a function of motor reference signals and motor terminal quantities, and
- Measurement of modified reactive power.

A fourth group, which uses extended Kalman filter for parameter estimation, may be added. General review for these different schemes can be found in Shieh *et al.* (1998), Ba-razzouk *et al.* (1999), Hren and Jezernik (1997), and Krishnan and Bharadwaj (1991). It is stated that the majority of the proposed schemes require intensive calculations to converge.

In this paper a simple estimator (which utilises only accessible variables for measurements such as voltages, currents and speed) based on two equations for the rotor flux estimation is presented. Similar approach of the proposed estimator with different adaptation algorithm was used (Marwali and Keyhani, 1997; Schauder, 1992) to estimate motor speed in a sensorless speed application, and the inverse rotor time constant (Shyu *et al.*, 1996). The proposed method is similar in its approach to that proposed by Shyu *et al.* (1996). However, apart from the difference in the algorithm for

obtaining the error adaptation signal, voltage phase sensors which were used along with a low pass filter to estimate rotor flux vector by Shyu *et al.* (1996), adding extra hardware complications, where eliminated in this work. Further, test results obtained by Shyu *et al.* (1996) were at a speed (approximately) of 17 per cent of rated speed, while in this work comparable results were obtained at speed of about 10 per cent of rated speed.

2. SIMULINK induction motor model and indirect rotor field orientation technique

The dynamic model of an induction motor is first presented in the stator reference frame by equations (1a) and (1b) as:

$$\vec{v}_{\mathrm{s}} = R_{\mathrm{s}}\vec{i}_{\mathrm{s}} + \frac{\mathrm{d}\vec{\lambda}_{\mathrm{s}}}{\mathrm{d}t} \tag{1a}$$

$$\vec{v}_{\mathrm{r}} = R_{\mathrm{r}}\vec{i}_{\mathrm{r}} + \frac{\mathrm{d}\vec{\lambda}_{\mathrm{r}}}{\mathrm{d}t} - j\omega_{\mathrm{r}}\vec{\lambda}_{\mathrm{r}} \tag{1b}$$

where the rotor voltage $\vec{v}_{\mathrm{r}}$ is zero in a shorted rotor windings. The rotor and the stator fluxes are given, respectively, as:

$$\vec{\lambda}_{\mathrm{s}} = L_{\mathrm{s}}\vec{i}_{\mathrm{s}} + L_{\mathrm{m}}\vec{i}_{\mathrm{r}} \tag{2a}$$

$$\vec{\lambda}_{\mathrm{r}} = L_{\mathrm{m}}\vec{i}_{\mathrm{s}} + L_{\mathrm{r}}\vec{i}_{\mathrm{r}} \tag{2b}$$

substituting from equations (2a) and (2b) into equations (1a) and (1b) and resolving the resultant two equation on the stator stationary reference frame dq gives:

$$\left\{\begin{array}{l} i_{\mathrm{sd}} = \frac{1}{SL_{\mathrm{s}}}(v_{\mathrm{sd}} - SL_{\mathrm{m}}i_{\mathrm{rd}} - R_{\mathrm{s}}i_{\mathrm{sd}}) \\ i_{\mathrm{sq}} = \frac{1}{SL_{\mathrm{s}}}(v_{\mathrm{sq}} - SL_{\mathrm{m}}i_{\mathrm{rq}} - R_{\mathrm{s}}i_{\mathrm{sq}}) \\ i_{\mathrm{rd}} = \frac{1}{SL_{\mathrm{r}}}(-SL_{\mathrm{m}}i_{\mathrm{sd}} - \omega_{\mathrm{r}}L_{\mathrm{m}}i_{\mathrm{sq}} - \omega_{\mathrm{r}}L_{\mathrm{r}}i_{\mathrm{rq}} - R_{\mathrm{r}}i_{\mathrm{rd}}) \\ i_{\mathrm{rq}} = \frac{1}{SL_{\mathrm{r}}}(\omega_{\mathrm{r}}L_{\mathrm{m}}i_{\mathrm{sd}} - SL_{\mathrm{m}}i_{\mathrm{sq}} + \omega_{\mathrm{r}}L_{\mathrm{r}}i_{\mathrm{rd}} - R_{\mathrm{r}}i_{\mathrm{rq}}) \end{array}\right\} \tag{3}$$

To complete the model the electrical speed of the rotor ω_{r} can be computed from the electromechanical equations of the motor as given by equations (4) and (5):

$$T_{\mathrm{em}} = \frac{3PL_{\mathrm{m}}}{4}(i_{\mathrm{sq}}i_{\mathrm{rd}} - i_{\mathrm{sd}}i_{\mathrm{rq}}) \tag{4}$$

and

$$\frac{\mathrm{d}\omega_{\mathrm{m}}}{\mathrm{d}t} = -\frac{B}{J}\omega_{\mathrm{m}} + \frac{T_{\mathrm{em}} - T_{\mathrm{L}}}{J} \tag{5}$$

where ω_{m} in equation (5) is the mechanical speed of the rotor in rad/s and is given in terms of the electrical speed of the rotor as:

$$\frac{P}{2}\omega_{\mathrm{m}} = \omega_{\mathrm{r}} \tag{6}$$

The SIMULINK model for an induction motor in the stator reference frame is shown in Figure 1. Note that in a practical machine the rotor currents are not measurable and can be estimated by a state observer.

In a field oriented control (FOC) drive, the control part is usually performed in the (a synchronously rotating) DQ reference frame for simplicity, where reference signals for torque and flux are set, and then converted in real time into variable like currents and voltages to be fed to the motor in the stator reference frame (Trzynadlowski, 1994). IRFOC typically is performed in the rotor reference frame, and in order to drive the reference signals in that reference frame, the dynamic model of a three-phase induction motor with a squirrel-cage rotor is redefined by vector equations expressed in DQ reference frame, which is aligned with rotor flux vector and rotates at a speed ω_e, as:

$$\vec{v}_{\mathrm{s}}^{e} = R_{\mathrm{s}}\vec{i}_{\mathrm{s}}^{e} + \frac{\mathrm{d}\vec{\lambda}_{s}^{e}}{\mathrm{d}t} + j\omega_e\vec{\lambda}_{s}^{e} \tag{7a}$$

$$\vec{0} = \vec{R}_{\mathrm{r}}\vec{i}_{\mathrm{r}}^{e} + \frac{\mathrm{d}\vec{\lambda}_{\mathrm{r}}^{e}}{\mathrm{d}t} - j(\omega_e - \omega_{\mathrm{r}})\vec{\lambda}_{\mathrm{r}}^{e} \tag{7b}$$

and equations (2a) and (2b) in the DQ reference frame becomes:

$$\vec{\lambda}_{\mathrm{s}}^{e} = L_{\mathrm{s}}\vec{i}_{\mathrm{s}}^{e} + L_{\mathrm{m}}\vec{i}_{\mathrm{r}}^{e} \tag{8a}$$

$$\vec{\lambda}_{\mathrm{r}}^{e} = L_{\mathrm{m}}\vec{i}_{\mathrm{s}}^{e} + L_{\mathrm{r}}\vec{i}_{\mathrm{r}}^{e} \tag{8b}$$

Similarly, the developed torque can be expressed using the stator current and rotor flux in the DQ rotating reference frame as:

$$T_{\mathrm{em}} = \frac{3}{4}\frac{L_{\mathrm{m}}}{L_{\mathrm{r}}}P(i_{\mathrm{SQ}}\lambda_{\mathrm{RD}} - i_{\mathrm{SD}}\lambda_{\mathrm{RQ}}) \tag{9}$$

The main objective of the field oriented control is to convert the control of torque production in induction motor in a similar manner to separately excited DC motor, where the torque and the flux in the motor can be controlled independently. Induction motors are single input terminal devices (in case of shorted rotor) and to obtain an independent control over the torque and the flux produced in the motor, the stator current is normally decoupled into two components, however, the decoupling cannot be obtained in a straightforward manner. The coupling between the stator's Q and D current components can be seen when substituting for the rotor current vector in equation (7b) from equation (8b), thus:

$$S\vec{\lambda}_{\mathrm{r}}^{e} = \frac{1}{\tau_{\mathrm{r}}}\left\{L_{\mathrm{m}}\vec{i}_{\mathrm{s}}^{e} - (1 + j\tau_{\mathrm{r}}\omega_{\mathrm{sl}})\vec{\lambda}_{\mathrm{r}}^{e}\right\} \tag{10}$$

where τ_{r} is the rotor time constant ($= L_{\mathrm{r}}/R_{\mathrm{r}}$), ω_{sl} is the slip frequency ($= (\omega_e - \omega_{\mathrm{r}})$) and S is the Laplace operator ($= \mathrm{d}/\mathrm{d}t$).

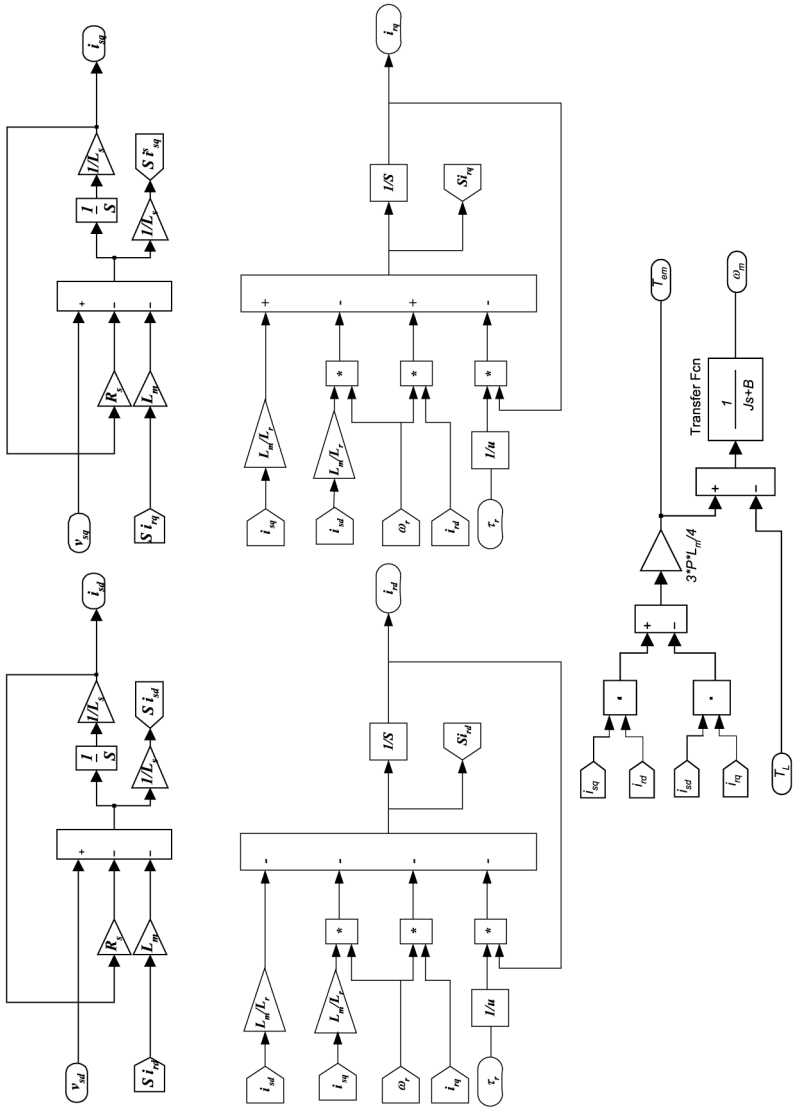

Figure 1.
Induction motor model
using SIMULINK

Equation (10) can be separated into two components D and Q as:

$$S\lambda_{RD} = \frac{L_m}{\tau_r} i_{SD} - \frac{\lambda_{RD}}{\tau_r} + \omega_{sl}\lambda_{RQ} \tag{11a}$$

$$S\lambda_{RQ} = \frac{L_m}{\tau_r} i_{SQ} - \frac{\lambda_{RQ}}{\tau_r} - \omega_{sl}\lambda_{RD} \tag{11b}$$

Terms $\omega_{sl}\lambda_{RQ}$ in equation (11a) and $\omega_{sl}\lambda_{RD}$ in equation (11b) cause cross coupling between the DQ components of the stator currents. The cross coupling can be eliminated by forcing either λ_{RD} or λ_{RQ} to be zero. If it is selected that $\lambda_{RQ} = 0$, then this requires that *D*-axis of the DQ rotating frame to be aligned with the rotor flux vector (Trzynadlowski, 1994) and thus $\lambda_{RD} = \lambda_r^*$ becomes a reference command signal. Under this condition, the induction motor becomes a linear current to torque converter. Setting $\lambda_{RQ} = 0$ in equation (9) shows that the torque is linearly proportional to i_{SQ}.

However, in a variable speed drive application speed is usually sought as an input variable as shown in Figure 2. Therefore, motor speed (ω_m) is measured and compared with reference speed (ω_m^*). The error signal produced is usually regulated using a PI controller to produce the reference torque command to a FOC drive as:

$$T^* = K_P(\omega_m^* - \omega_m) + K_I \int (\omega_m^* - \omega_m)dt \tag{12}$$

Now if the input torque command to the motor (T^*) is available from equation (12), then the reference quadrature component of the stator current to be supplied to the motor (i_{SQ}^*) can be obtained as:

$$i_{SQ}^* = \frac{4L_r}{3PL_m}\frac{T^*}{\lambda_r^*} \tag{13}$$

If the motor is considered to be operating in the constant flux region (below the base speed) where the flux of the machine is typically maintained to its nominal value for operation below the base speed, then the reference direct component of the motor stator current (i_{SD}^*) can be obtained from equation (11a) by setting $\lambda_{RQ} = 0$, $\lambda_{RD} = \lambda_r^*$, and in steady state of the motor ($S = 0$) as:

$$i_{SD}^* = \frac{\lambda_r^*}{L_m} \tag{14}$$

Once the reference currents i_{SQ}^* and i_{SD}^* are obtained, they are compared with the motor currents and the error signal produced is fed to current PI controllers in order to generate the command voltages as in case of a VSI fed induction motor. Noting that the motor currents are measured in stationary stator dq reference frame and the reference command currents are produced, as in equations (11a) and (11b), in synchronously rotating DQ reference frame. This requires transforming the motor measured currents to the DQ reference frame as shown in Figure 2. The dq-to-DQ transformation requires the knowledge of the rotor flux vector position, i.e. angle θ, which can be obtained as:

$$\theta = \theta_r + \int \omega_{sl}^* dt \tag{15}$$

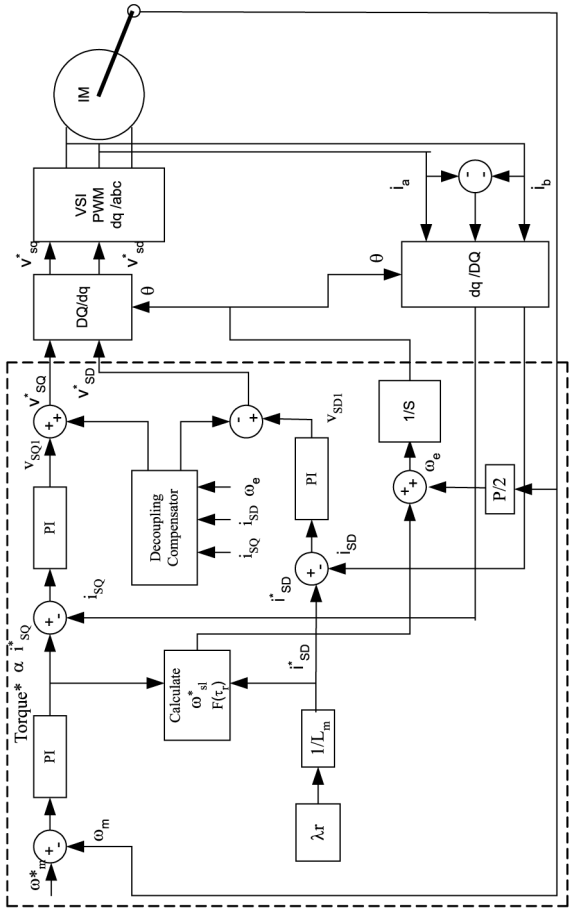

Figure 2.
Block diagram for IRFOC system

θ_r (rotor angular position) can easily be determined by measuring the motor mechanical speed using an optical encoder, but ω_{sl}^* (reference slip angular velocity) needs to be estimated.

The command slip frequency can be found from equation (11b), by substituting $\lambda_{RQ}^e = 0$, and $\lambda_{RD} = \lambda_r^*$, thus ω_{sl}^* is given as:

$$\omega_{sl}^* = \frac{L_m}{\tau_r}\frac{i_{SQ}^*}{\lambda_r^*} \tag{16}$$

Equation (16) shows that ω_{sl}^* is dependent on the motor parameter such as L_m and τ_r. It is found that τ_r is difficult to be accurately measured (due to the fact that the rotor is not easily accessible), and the most likely parameter to change with temperature. Therefore, accurate knowledge of τ_r is one of the essential factors for success of IFOC (Ouhrouche and Volat, 2000).

In an IFOC there are also two current controllers responsible for producing the D and Q voltage signals for the stator of the motor. Expressing the stator voltage in equation (7a) in terms of the stator current and rotor flux from equations (8a) and (8b):

$$\vec{v}_s^e = (R_s + (S + j\omega_e)\sigma L_s)\vec{i}_s^e + (S + j\omega_e)\frac{L_m}{L_r}\vec{\lambda}_r^e \tag{17}$$

where $\sigma = 1 - (L_m^2/L_rL_s)$. Decomposing equation (17) into D and Q terms gives the stator voltages in the DQ rotating reference frame as:

$$v_{SD} = (R_s + S\sigma L_s)i_{SD} - \omega_e\sigma L_s i_{SQ} + S\frac{L_m}{L_r}\lambda_{DR} - \omega_e\frac{L_m}{L_r}\lambda_{RQ} \tag{18a}$$

$$v_{SQ} = (R_s + S\sigma L_s)i_{SQ} + \omega_e\sigma L_s i_{SD} + S\frac{L_m}{L_r}\lambda_{RQ} + \omega_e\frac{L_m}{L_r}\lambda_{RD} \tag{18b}$$

setting $\lambda_{RQ} = 0$, and $\lambda_{RD} = \lambda_r^*$ in equations (18a) and (18b) gives:

$$R_s i_{SD} + S\sigma L_s i_{SD} = v_{SD} + \omega_e\sigma L_s i_{SQ} \tag{19a}$$

$$R_s i_{SQ} + S\sigma L_s i_{SQ} = v_{SQ} - \omega_e\left\{\sigma L_s i_{SD} + \frac{L_m}{L_r}\lambda_r^*\right\} \tag{19b}$$

If the current i_{SD} in equation (19a) is considered the input command signal (i_{SD}^*) to the *D*-axis PI stator current controller, then the output of the controller in response to this input will be v_{SD}^*. Similar input-output relationship is considered for the Q-axis PI stator current controller, where i_{SQ}^* is the reference input to the controller and v_{SQ}^* is the output response.

However, coupling exists between equations (19a) and (19b). The two equations can be decoupled by introducing new variables v_{SD1} and v_{SQ1} (Benhaddadi *et al.*, 1997):

$$R_s i_{SD}^* + S\sigma L_s i_{SD}^* = v_{SD1} \quad \text{(PI output)} \tag{20a}$$

$$R_s i_{SQ}^* + S\sigma L_s i_{SQ}^* = v_{SQ1} \quad \text{(PI output)} \tag{20b}$$

To compensate for the error introduced when decoupling equations (19a) and (19b), the values of v_{SD1}, and v_{SQ1} are corrected, as shown in Figure 2, in order to give the correct reference voltages v_{SD}^* and v_{SQ}^* as:

$$v_{SD1} - \omega_e \sigma L_s i^*_{SQ} = v^*_{SD} \tag{21a}$$

$$v_{SQ1} + \omega_e \left\{ \sigma L_s i^*_{SD} + \frac{L_m}{L_r} \lambda^*_r \right\} = v^*_{SQ} \tag{21b}$$

Figure 3 shows the SIMULINK block diagram for part of the IRFOC in the dashed box.

3. Rotor time constant estimator

The estimator for the inverse of the rotor time constant is designed to serve two purposes, which are obtaining a correct initial estimation and to track the changes in the rotor time constant on the motor side. It uses error signal generated from the difference between two equations used to estimate the rotor flux in the stator reference frame. Figure 4 shows the updated algorithm of the inverse rotor time constant.

As the variables used by this estimator are signals measured directly from the stator terminals (i.e. currents and voltages), it will be more convenient to design the estimator with its variables in the stator reference frame. Therefore, equation (1b) is rewritten in terms of the rotor flux and the stator current by substituting for the rotor current from equation (2b) as:

$$\vec{v}_r = \vec{0} = R_r \left(\frac{\vec{\lambda}_r - L_m \vec{i}_s}{L_r} \right) + (S - j\omega_r)\vec{\lambda}_r \quad \text{rearranging,} \quad \vec{\lambda}_r = \frac{\hat{G}_r L_m}{(\hat{G}_r + (S - j\omega_r))} \vec{i}_s \tag{22}$$

where $\hat{G}_r$ is defined as the estimated inverse rotor time constant.

Equation (22) gives an estimation of the rotor flux in the stator reference frame. One should observe that signals and parameters used in equation (22) could be easily measured (i_s and ω_r) or calculated to a very good accuracy (such as L_m), however, $\hat{G}_r$ has to be estimated. Noting also that equation (22) is a function of $\hat{G}_r$, this permits using it as an adaptive model equation which can be adjusted for variations in $\hat{G}_r$. Another independent estimate of the rotor flux, which can be set as a reference equation, can be obtained from equation (1a), and by substituting for the stator flux vector in terms of the rotor flux vector from equations (2a) and (2b). This gives:

$$\begin{aligned} \vec{v}_s &= R_s \vec{i}_s + S \left\{ L_s \vec{i}_s + L_m \left(\frac{\vec{\lambda}_r - L_m \vec{i}_s}{L_r} \right) \right\} \quad \text{rearranging,} \\ \vec{\lambda}_r &= \frac{1}{S} \left\{ \frac{L_r}{L_m} (\vec{v}_s - (R_s + S\sigma L_s) \vec{i}_s \right\} \end{aligned} \tag{23}$$

Figure 5 shows the SIMULINK blocks for equations (22) and (23). Again it should be observed that equation (23) is not a function of inverse rotor time constant, and signals such as stator currents and voltages can be measured fairly accurate, particularly, at high frequency of stator currents. However, the estimator suggested in this paper uses the two estimated values of the rotor flux magnitude from equations (22) and (23). The error between the magnitudes of the two estimators is used an input to a linear PI controller which in turn produces the deviation in the inverse rotor time constant, thus for a small deviation, Δe can be written as:

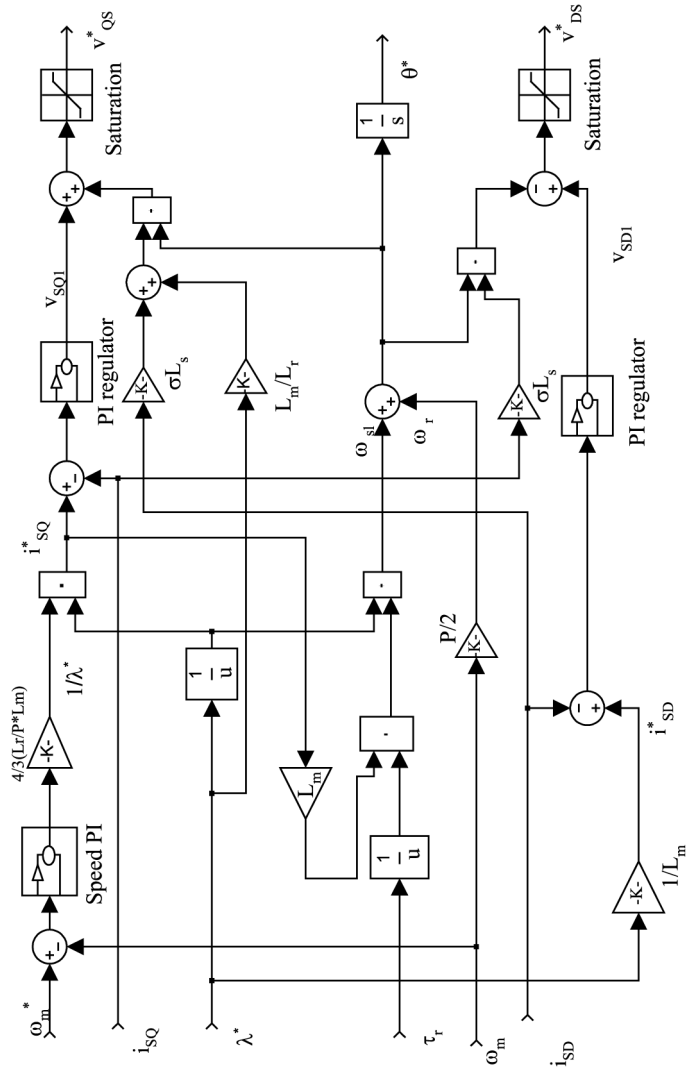

Figure 3.
IRFOC SIMULINK model

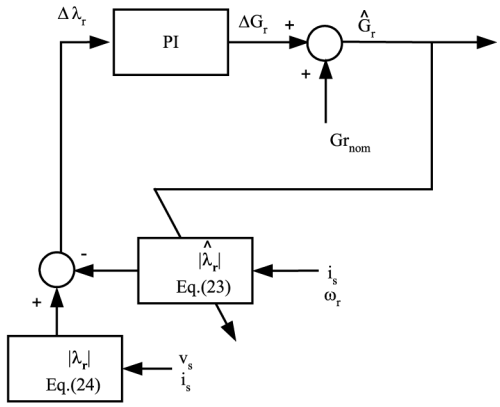

Figure 4.
Proposed estimator for inverse rotor time constant

$$\Delta e = \Delta|\lambda_r| - \Delta|\lambda_r^*| \tag{24}$$

where $|\lambda_r|$ and $|\lambda_r^*|$ are, respectively, the magnitudes of the reference and estimated rotor flux from equations (23) and (22). The amount of change in the inverse rotor time constant related to this error signal is:

$$\Delta G_r = k_{pGr}\Delta e + k_{iGr}\int \Delta e dt \tag{25}$$

where k_{pGr} and k_{iGr} are the proportional and integral gains of the inverse rotor time constant regulator. ΔG_r is the estimated change in the inverse rotor time constant and is fed back into equation (22) to adjust the initial value of the inverse rotor time constant.

When no error exists in the estimated inverse rotor time constant the two equations are supposed to give the same value of the rotor flux (hence the error is zero) and therefore the nominal value of the inverse rotor time constant is obtained. The nominal values of the motor parameters are used in equations (22) and (23) for initialisation. It can be seen that equations (22) and (23) are both dependent on L_m which in turn could produce an error between the two estimated values of the flux, however if the machine has to function in the constant flux region, where the flux is maintained to its nominal level, the inductances of the machine remain relatively constant to their nominal values and very lightly affected by the operating conditions of the machine (Ba-razzouk *et al.*, 1999; Halasz *et al.*, 1995; Nait and Benbouzid, 1999).

To investigate the dynamic response of the proposed inverse rotor time constant estimator, it is necessary to linearise equation (24) for a small deviation about a particular point. However, equation (22) is in stationary reference frame, and if the linearisation is done in a stationary reference frame, the resulting linear equations will still be time varying; therefore, it is useful to transform the equations to a reference frame rotating synchronously with the stator current vector, thus equation (22) is rewritten as:

$$\hat{\lambda}_r^e = \frac{\hat{G}_r \hat{L}_m}{(\hat{G}_r + (S - j(\omega_e - \hat{\omega}_r))} \hat{i}_s^e \tag{26}$$

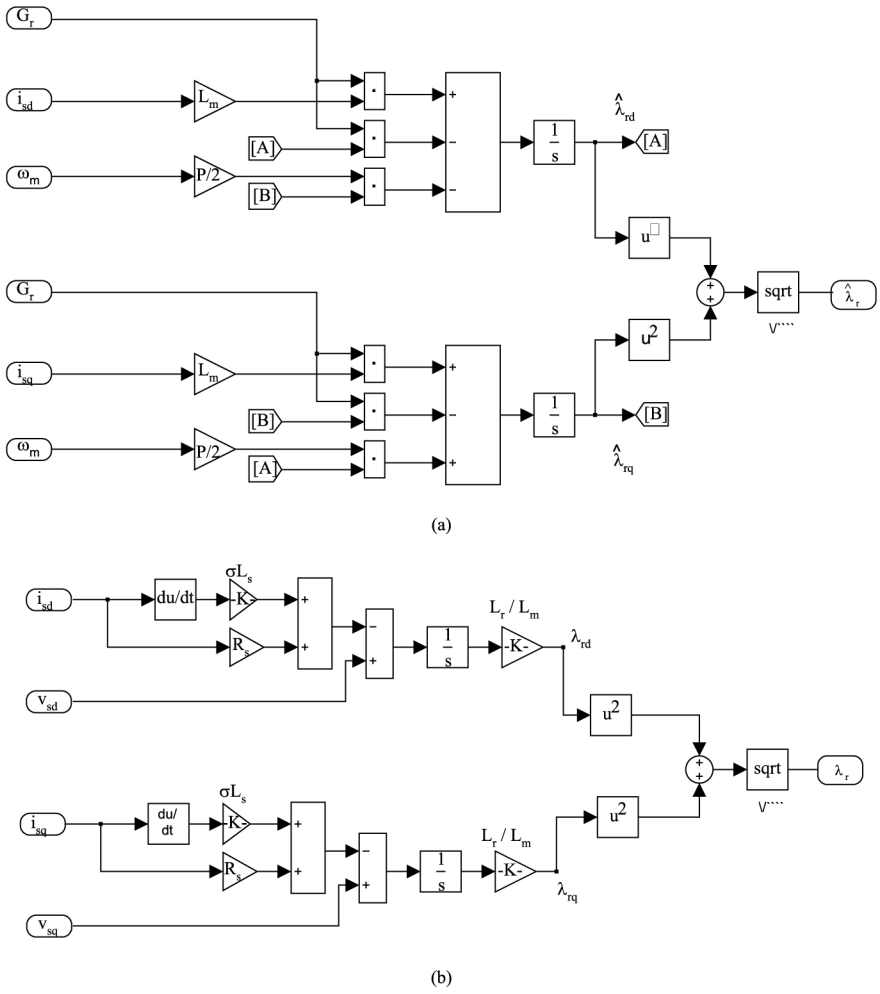

Figure 5.
Implementation of (a) adaptive and (b) reference equations

The magnitude of the estimated rotor flux vector in equation (26) can be expressed as:

$$|\hat{\vec{\lambda}}_{\mathrm{r}}^{e}| = |\lambda_{\mathrm{r}}| = \sqrt{(\hat{\lambda}_{\mathrm{RD}})^2 + (\hat{\lambda}_{\mathrm{RQ}})^2} \tag{27}$$

decomposing equation (26) into DQ components as:

$$\hat{\lambda}_{\mathrm{RD}} = \frac{\hat{G}_{\mathrm{r}}\hat{L}_{\mathrm{m}}}{(S + \hat{G}_{\mathrm{r}})}\hat{i}_{\mathrm{SD}} - \frac{(\omega_e - \hat{\omega}_{\mathrm{r}})}{(S + \hat{G}_{\mathrm{r}})}\hat{\lambda}_{\mathrm{RQ}} \tag{28a}$$

and

$$\hat{\lambda}_{RQ} = \frac{\hat{G}_r \hat{L}_m}{(S + \hat{G}_r)} \hat{i}_{SQ} + \frac{(\omega_e - \hat{\omega}_r)}{(S + \hat{G}_r)} \hat{\lambda}_{RD} \tag{28b}$$

and the amount of deviation $\Delta|\lambda_r|$ can be expressed using Taylor's series expansion around a working point as:

$$\begin{aligned} \Delta|\hat{\lambda}_r| &= \frac{\partial|\hat{\lambda}_r|}{\partial \hat{\lambda}_{RD}} \Delta\hat{\lambda}_{RD} + \frac{\partial|\hat{\lambda}_r|}{\partial \hat{\lambda}^*_{RQ}} \Delta\hat{\lambda}_{RQ} \\ \Delta|\hat{\lambda}_r| &= \frac{\hat{\lambda}_{RD}}{|\hat{\lambda}_r|} \Delta\hat{\lambda}_{RD} + \frac{\hat{\lambda}_{RQ}}{|\hat{\lambda}_r|} \Delta\hat{\lambda}_{RQ} \end{aligned} \tag{29}$$

and the terms $\Delta\hat{\lambda}_{RD}$ and $\Delta\hat{\lambda}_{RQ}$ in equation (29) can be obtained by expanding the terms in equations (28a) and (28b):

$$\Delta\hat{\lambda}_{RD} = \frac{\partial\hat{\lambda}_{RD}}{\partial\hat{G}_r}\Delta\hat{G}_r + \frac{\partial\hat{\lambda}_{RD}}{\partial\hat{\lambda}_{RQ}}\Delta\hat{\lambda}_{RQ} + \frac{\partial\hat{\lambda}_{RD}}{\partial\hat{\omega}_r}\Delta\hat{\omega}_r + \frac{\partial\hat{\lambda}_{RD}}{\partial\hat{i}_{SD}}\Delta\hat{i}_{SD} + \ldots \tag{30a}$$

$$\Delta\hat{\lambda}_{RQ} = \frac{\partial\hat{\lambda}_{RQ}}{\partial\hat{G}_r}\Delta\hat{G}_r + \frac{\partial\hat{\lambda}_{RQ}}{\partial\hat{\lambda}_{RD}}\Delta\hat{\lambda}_{RD} + \frac{\partial\hat{\lambda}_{RQ}}{\partial\hat{\omega}_r}\Delta\hat{\omega}_r + \frac{\partial\hat{\lambda}_{RQ}}{\partial\hat{i}_{SD}}\Delta\hat{i}_{SD} + \ldots \tag{30b}$$

During steady state, and for a given operating speed and load conditions, terms such as

$$\frac{\partial\hat{\lambda}_{RD}}{\partial\hat{\omega}_r}\Delta\hat{\omega}_r + \frac{\partial\hat{\lambda}_{RD}}{\partial\hat{i}_{SD}}\Delta\hat{i}_{SD}$$

in equation (30a) and

$$\frac{\partial\hat{\lambda}_{RQ}}{\partial\hat{\omega}_r}\Delta\hat{\omega}_r + \frac{\partial\hat{\lambda}_{RQ}}{\partial\hat{i}_{SD}}\Delta\hat{i}_{SD}$$

in equation (30b) can safely be set to zero. Further, the term which involves $\Delta\hat{L}_m$ can also be set to zero considering the $L_m = \hat{L}_m =$ nominal value of the motor inductance L_{mo} also the estimated stator currents and speed can be set to their actual values in equations (28a) and (28b) as these quantities are directly measured (i.e. $\hat{i}_{SD} = i_{SD}$, $\hat{i}_{SQ} = i_{SQ}$, and $\hat{\omega}_r = \omega_r$). Thus equations (30a) and (30b) can be reduced to:

$$\Delta\hat{\lambda}_{RD} = \frac{\partial\hat{\lambda}_{RD}}{\partial\hat{G}_r}\Delta\hat{G}_r + \frac{\partial\hat{\lambda}_{RD}}{\partial\hat{\lambda}_{RQ}}\Delta\hat{\lambda}_{RQ} \tag{31a}$$

and

$$\Delta\hat{\lambda}_{RQ} = \frac{\partial\hat{\lambda}_{RQ}}{\partial\hat{G}_r}\Delta\hat{G}_r + \frac{\partial\hat{\lambda}_{RQ}}{\partial\hat{\lambda}_{RD}}\Delta\hat{\lambda}_{RD} \tag{31b}$$

evaluating equations (31a) and (31b) and substituting in equation (29) gives the following transfer function:

$$\frac{\Delta|\lambda_r^*|}{\Delta G_r} = \frac{KS((S+G_{ro})^2+\omega_{slo}^2) + (S+G_{ro})\omega_{slo}^2(\lambda_{ro})^2}{|\lambda_{ro}|(S+G_{ro})^2((S+G_{ro})^2+\omega_{slo}^2)} \tag{32}$$

where $K = (\lambda_{RDo}i_{DSo} + \lambda_{RQo}i_{SQo})$, $|\lambda_{ro}| = |\lambda_r^*| = \sqrt{\lambda_{RDo}^2 + \lambda_{RQo}^2}$, and $\omega_{slo} = (\omega_e - \omega_{ro})$. And it is assumed that $\hat{\lambda}_{RD} = \lambda_{RDo}$, $\hat{\lambda}_{RQ} = \lambda_{RQo}$, $\hat{i}_{SD} = i_{SDo}$, $\hat{i}_{SQ} = i_{SQo}$, and $\omega_r = \omega_{ro}$, for selected operating points.

The above transfer function in equation (32) is incorporated in a closed loop system as shown in Figure A1 to investigate its dynamic response. The denominator of equation (32) shows that the system is always stable, as it always has its poles in the left side of the *S*-plane. Root locus plots for the transfer function in equation (32), using the parameters given for the 0.37 kW in Appendix 1, were produced for two different operating points. Figure A2 in Appendix 3, shows the root locus when motor is running at nominal speed, and the other plot in Figure A3 is produced when the motor operation is extended near zero speed operation. Figure A2 shows that the system is stable for any selected gain. However, the low speed plot in Figure A3 shows that the system becomes unstable if the system gain (k_o) is selected such as $k_{c1} < k_o < k_{c2}$ where k_{c1} and k_{c2} are two critical for which the system becomes marginally stable and starts to oscillate. Using Ziegler-Nichols tuning approach, k_{c1} is selected as a critical gain k_{czn}, and thus optimal values for the gains k_{pGr} and k_{iGr} of the inverse rotor time constant regulator are obtained. The values of k_{pGr} and k_{iGr} used in this simulation for the 0.37 kW motor are 4.5 and 230, respectively, and for the 7.5 kW motor are 0.30 and 35.

4. Implementation issues

The practical implementation of the reference model in equation (23) on the DSP board is difficult, due to the required pure integration. This leads to problems with initial conditions and drift. Moreover, equation (23) is a function of the stator resistances R_s, which is expected to be affected by the operating temperature in a similar manner as the rotor resistance. The effect of an error in R_s is usually quite negligible at high excitation frequency but becomes more serious as the frequency approaches zero. However, one can always obtain good measurement of R_s; as the stator terminals are easily accessible (Sullivan *et al.*, 1996; Jang and Holtz, 1997; Robyns *et al.*, 1999; Toliyat *et al.*, 1999). To avoid such problems, a low pass filter, which has a pole very near to the origin, is normally used in place of pure integration. The implementation of the low pass filter is proposed in Marwali and Keyhani (1997), Schauder (1992), and Idris *et al.* (2001), where an identical linear transfer matrix is inserted in both the reference and adjustable model equations. However, this method requires extra hardware to be added to the controller circuit (voltage transducers), and it will introduce phase shift and the measurement can also suffer from inherent inaccuracy of the voltage transducer, especially at low voltage. Therefore, the terminal voltages of the inverter are estimated from the PWM signals

applied at the gates of the power devices and the DC link voltage, with dead time compensation as proposed in Yu *et al.* (2000) and Choi *et al.* (1996). The existing circuit for protection/detection of the DC link voltage on the MCK243 is used for this purpose.

5. Simulation and experimental results

Two motors are used in this study, one is 7.5 kW (Shi *et al.*, 1997), and the other is 0.37 kW supplied by Technosoft S.A. The motors parameters are given in Appendix 1. Different operating conditions are simulated to illustrate the operation of the estimator, and the effect of the rotor time constant mismatch on the IRFOC drive. The simulation is carried out using SIMULINK-MATLAB ver5.3.1.The parameters are fixed step of 0.0001 s and ode5 (Dormand-Prince) solver.

Figure 6 shows the simulation results for motor speed, torque, flux, and inverse rotor time constant estimation under rated conditions. The rotor time constant is initially underestimated by 50 per cent of the nominal value ($\tau_{\mathrm{r\,nom}} = 0.267$). The simulation is carried by starting the vector controlled drive to reach the rated speed, and continues for another 2 s, and then reverses the speed under rated load. The figure clearly shows that, the torque and flux dynamic responses are severely affected by the mismatch in the rotor time constant, and produced a slower response, and strong oscillations when compared with the one using the estimator.

The estimator is tested for low speeds at about 10 per cent of the rated speed, and τ_{r} is initially underestimated by 50 per cent. Simulation results in Figure 7 shows good stability, faster response in tracking the reference speed when using the estimator. Accuracy of estimator is demonstrated, where the estimator converges to the correct value in less than 1 s. The simulation results in Figures 6 and 7 confirm to the fact that the motor is under fluxed due to wrong estimation of the rotor time constant, which means that the machine is not efficiently used (Benhaddadi *et al.*, 1997).

Figures 8 and 9 show corresponding simulation results obtained using the 0.37 kW machine and when operated at 291.4 and 10 rad/s, respectively.

Figure 10 shows the simulation results for the case where the rotor time constant is initially overestimated by 100 per cent. Here the motor appears to be over fluxed. Over fluxing can cause saturation and increases the machine losses. Figure 11 shows the simulation results under similar conditions for the 0.37 kW motor.

An experimental study was carried out on the MCK243 development board (based around TMS320F243), which includes an intelligent three-phase inverter module ACPM750 supplied by Technosoft S.A. to verify the operation of the proposed estimator.

The 0.37 kW motor is used in the experimental set up. Figure 12 shows the speed and torque current responses for a step in the reference speed from 31.4 to 235.6 rad/s. Figure 13 shows the estimated rotor flux and inverse rotor time constant. Figure 13 shows successful estimation of the rotor flux and inverse rotor time constant at low speed (5 Hz), before the step application, and robustness towards speed variation (except for a small perturbation during the transient change in the speed). To demonstrate the effect of load change on the estimator operation, a step in load torque under constant reference speed is achieved when the drive is loaded with a separately excited DC generator. The motor was allowed to run at a speed of 235.6 rad/s while the generator's terminal is open circuit. A resistive load is plugged (by a manual switch) at the generator's terminal using to cause the required disturbance in the load torque. Speed and the corresponding

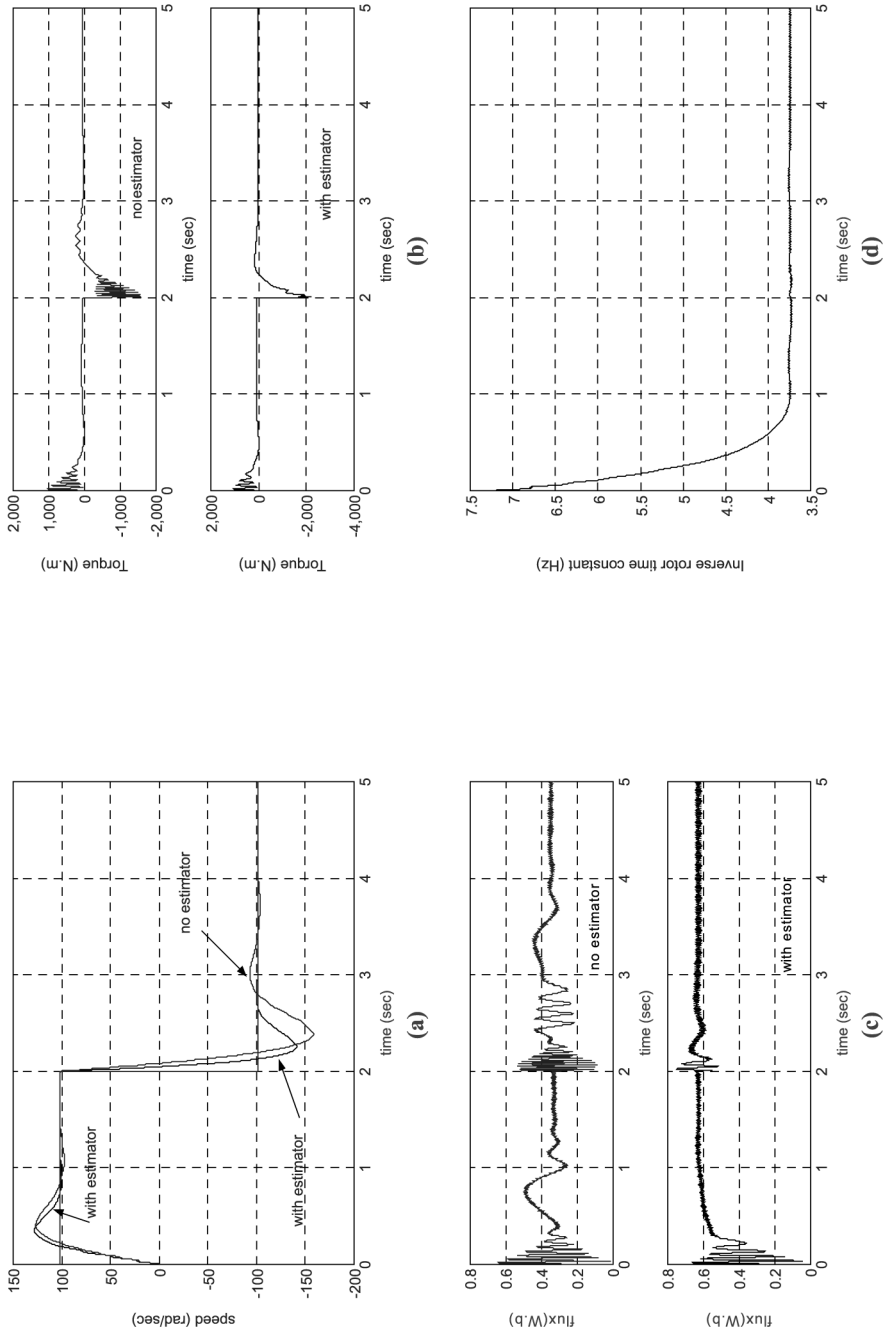

Figure 6.
7.5 kW motor (a) speed, (b) torque, (c) flux, and (d) inverse rotor time constant estimation vs time. Rated speed, rated torque and τ_r initially underestimated by 50 per cent

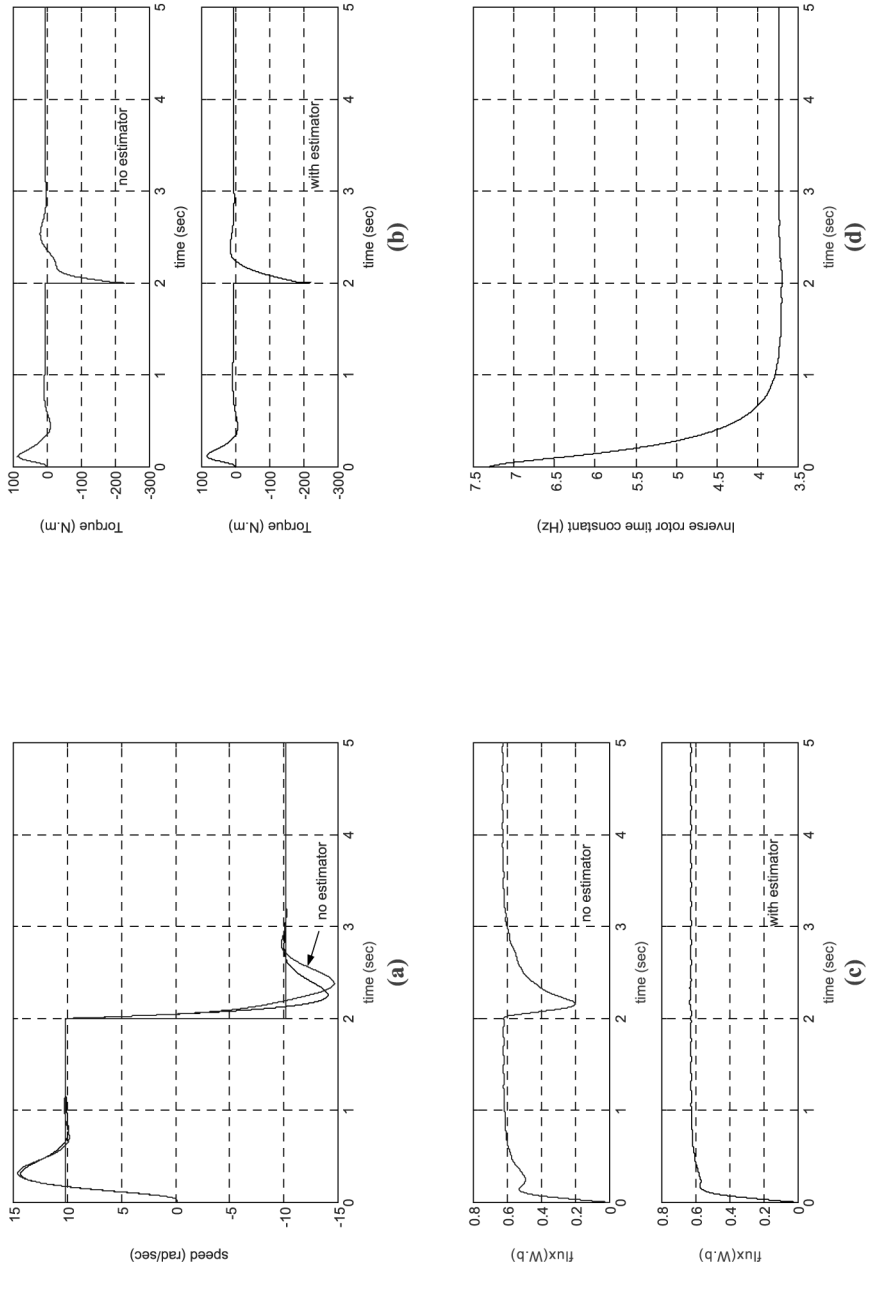

Figure 7.
7.5 kW motor (a) speed, (b) torque, (c) flux, and (d) inverse rotor time constant estimation vs time for10 per cent of the rated speed and τ_r initially underestimated by 50 per cent

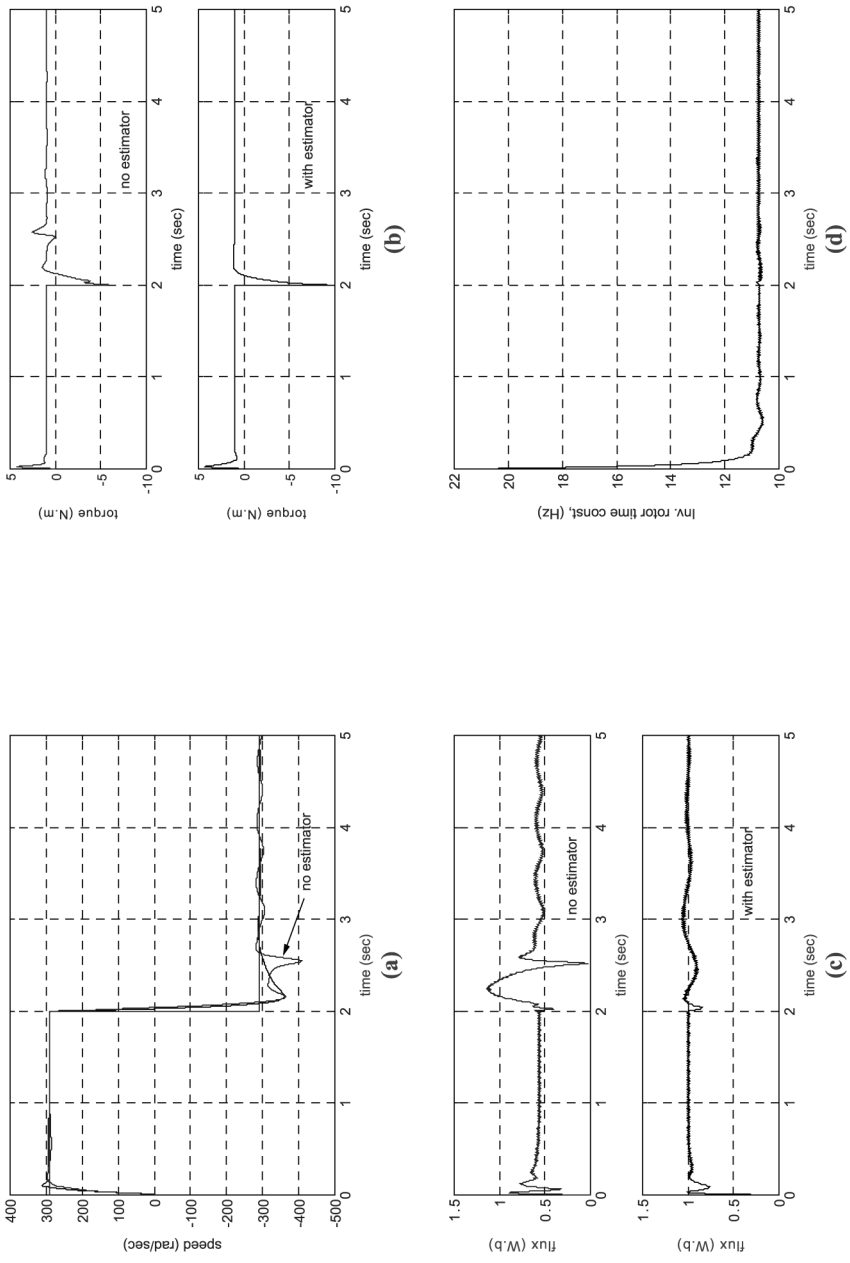

Figure 8.
0.37 kW motor (a) speed, (b) torque, (c) flux, and (d) inverse rotor time constant estimation vs time. Rated speed, rated torque and τ_r initially underestimated by 50 per cent

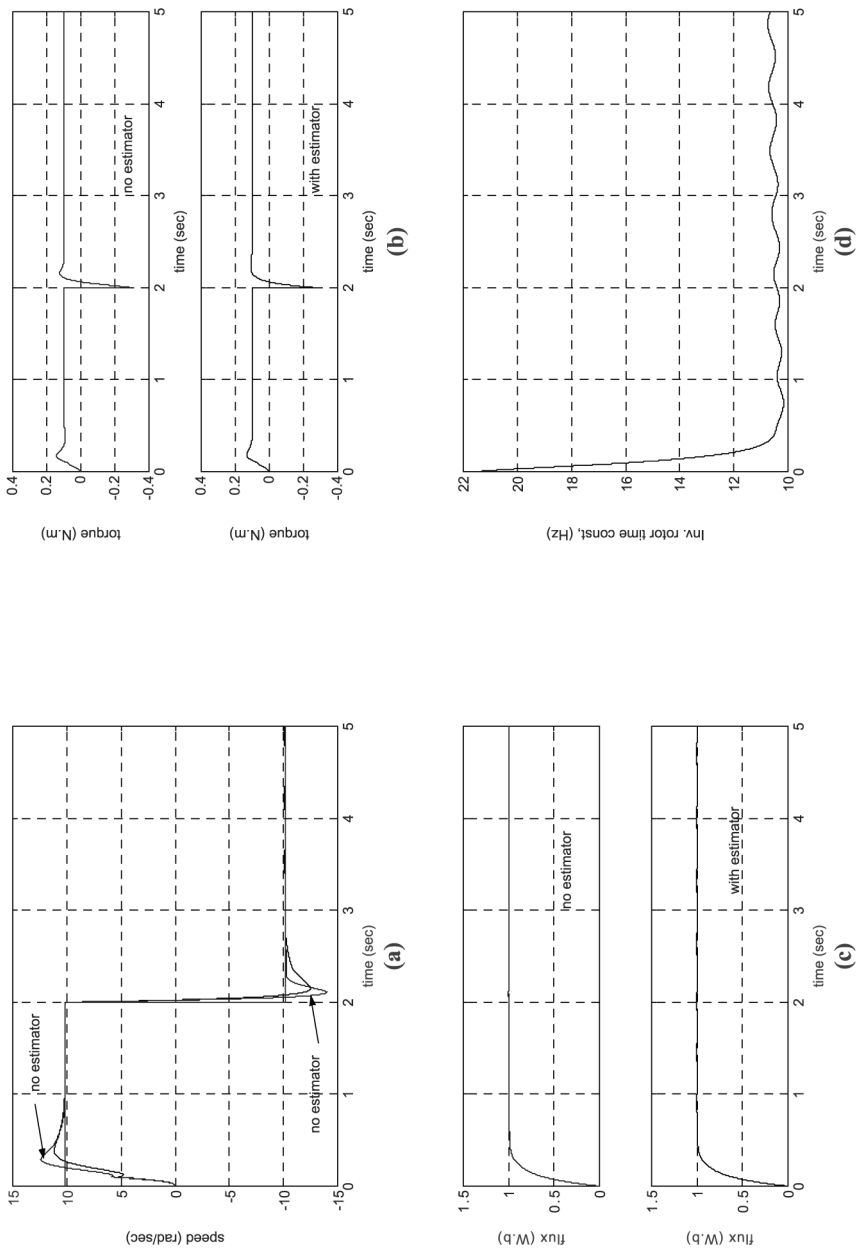

Figure 9.
0.37 kW motor (a) speed, (b) torque, (c) flux, and (d) inverse rotor time constant estimation vs time for 5 per cent of the rated speed and τ_r initially underestimated by 50 per cent

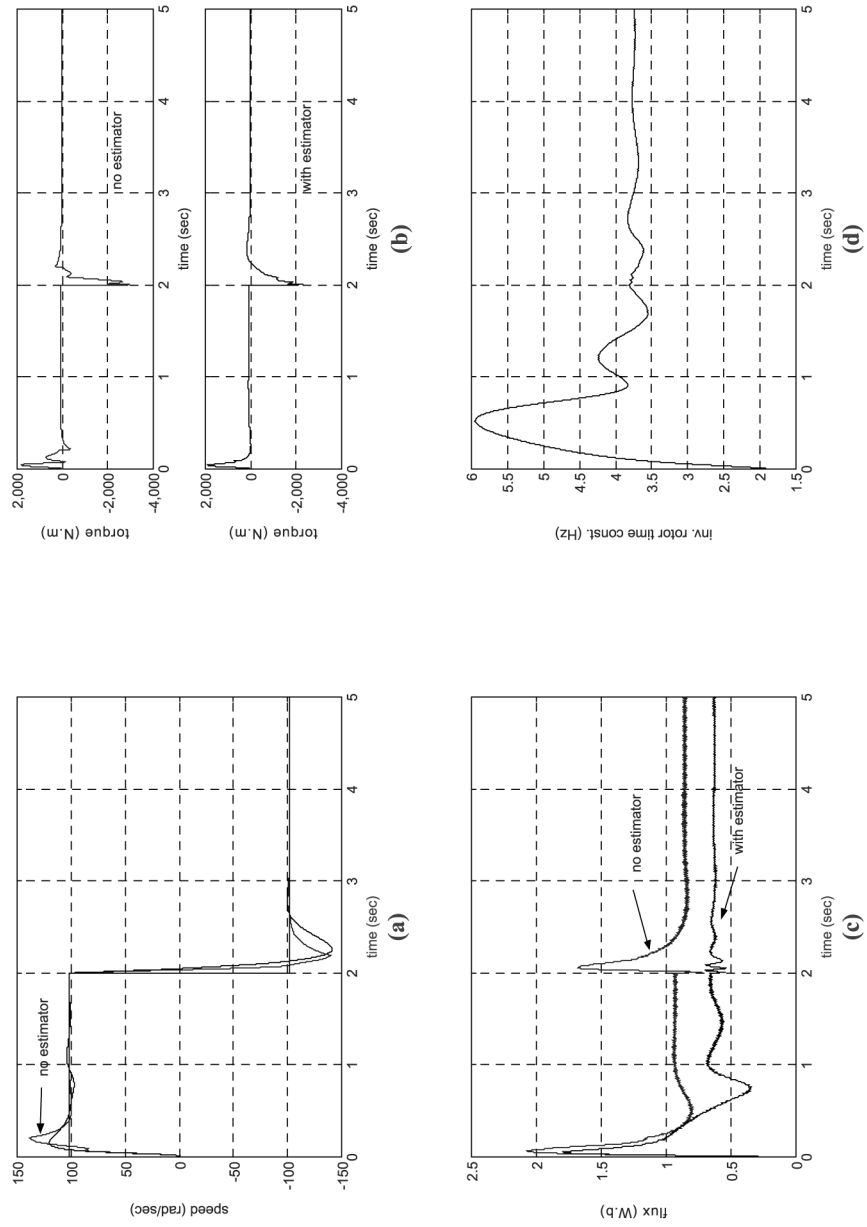

Figure 10.
7.5 kW motor (a) speed, (b) torque, (c) flux, and (d) inverse rotor time constant estimation vs time. Rated speed, rated torque and τ_r initially overestimated by 100 per cent

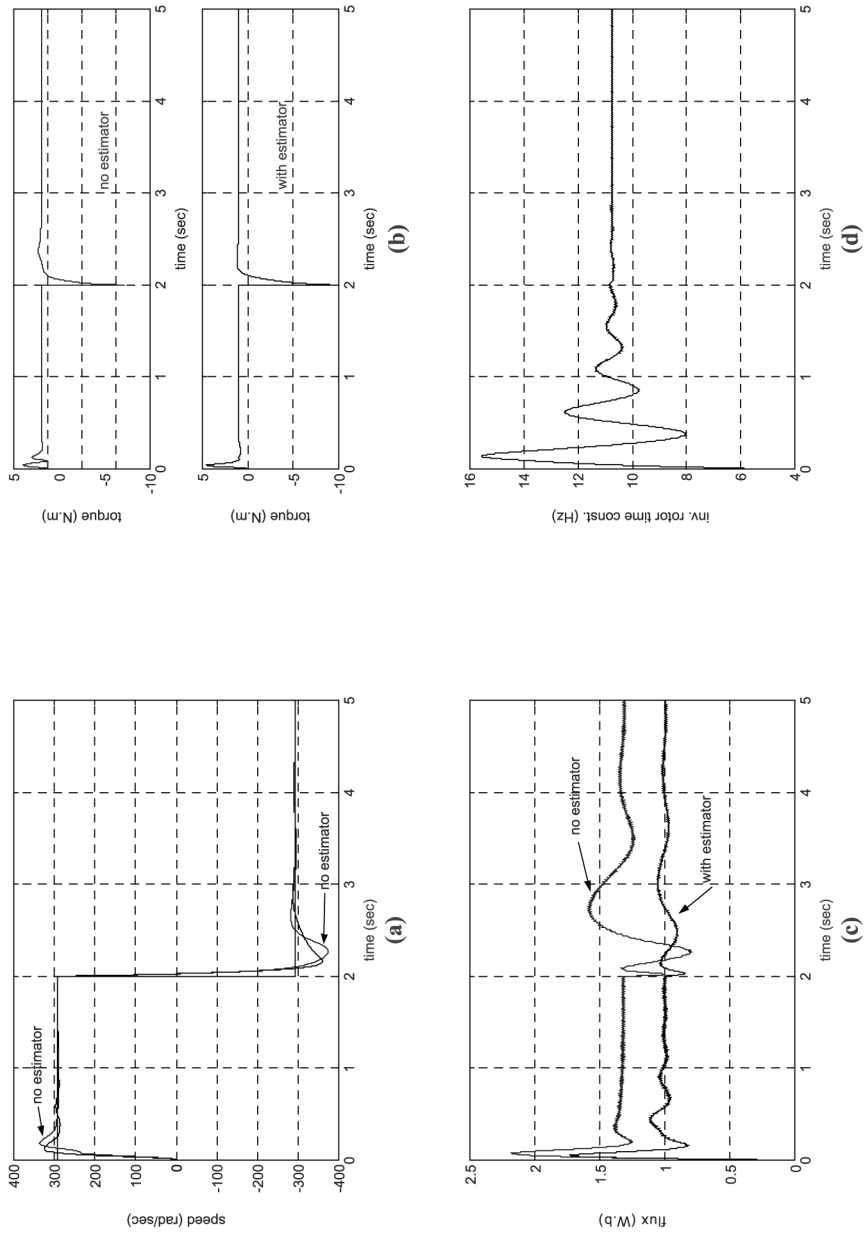

Figure 11.
0.37 kW motor (a) speed, (b) torque, (c) flux, and (d) inverse rotor time constant estimation vs time. Rated speed, rated torque, and τ_r initially overestimated by 100 per cent

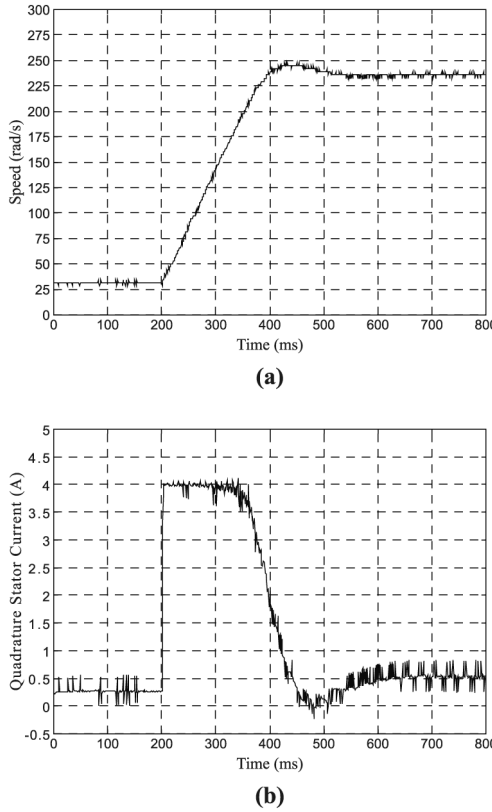

Figure 12.
Step change in reference speed from 31.4 to 235.6 rad/s under no load (experimental): (a) Speed and (b) Current (i_{SQ})

torque current responses are shown in Figure 14. The estimated inverse rotor time constant is shown in Figure 15.

6. Conclusion

The proposed estimator of inverse rotor time constant is successfully implemented and demonstrated in this study. The estimator used only those quantities available from the motor terminals, and it does not add any kind of expensive sensors or complicated calculation algorithms to an existing IRFOC drive. The identification scheme used in this paper demonstrated the validity of the method for both steady state and transient operation, and for a wide range of speeds (from rated to as low as 10 per cent).

The estimator output showed initial oscillation but finally reached to the steady state value of the inverse rotor time constant when the rotor time constant is initially over estimated. Finally, it is worth mentioning that results obtained from simulation and experimental work were found to be in a very good agreement except for small variation such as, an amount of noise existed in the measured quantities due to the switching frequencies of the VSI PWM source. However, in the simulation work this

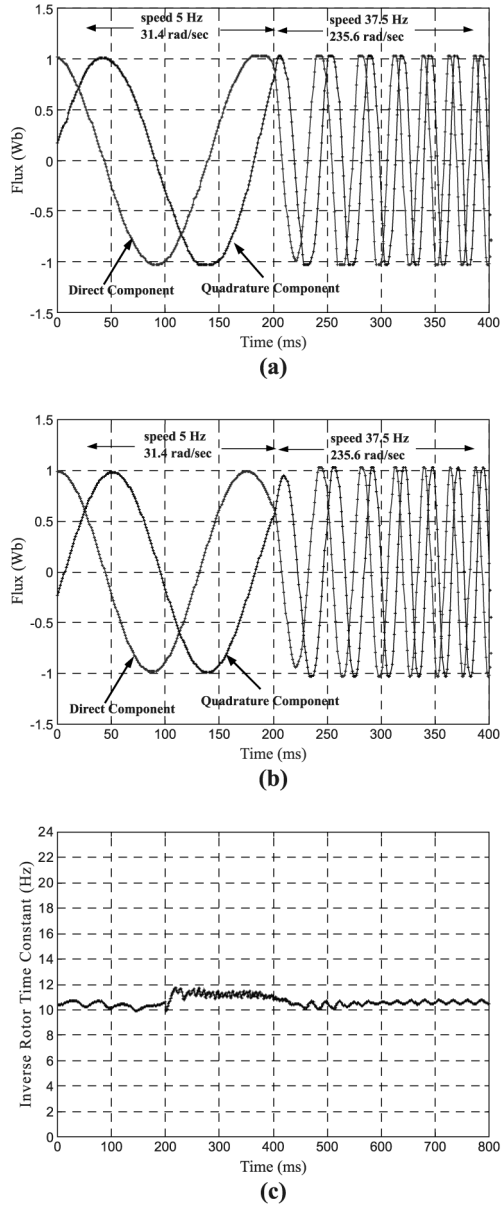

Figure 13.
Experimental estimation of direct and quadrature rotor flux (experimental) from: (a) Stator, (b) Rotor quantities, and (c) inverse rotor time constant ($\approx$ 10.74 Hz) under step change in reference speed from 31.4 to 235.6 rad/s under no load

(VSI PWM source) was considered as a linear supply produced by the vector controller (Wade *et al.*, 1997). In the simulation work as well, the speed is sensed without considering the effects of the differentiation, which takes a place to obtain the speed from the optical encoder position, on the experimental side.

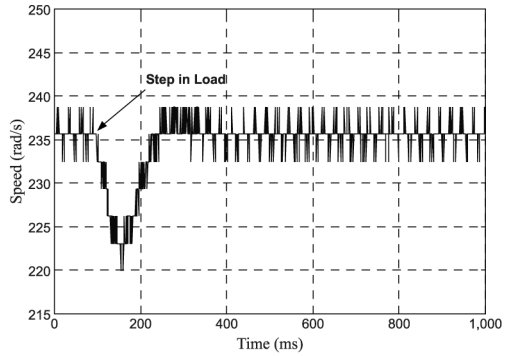

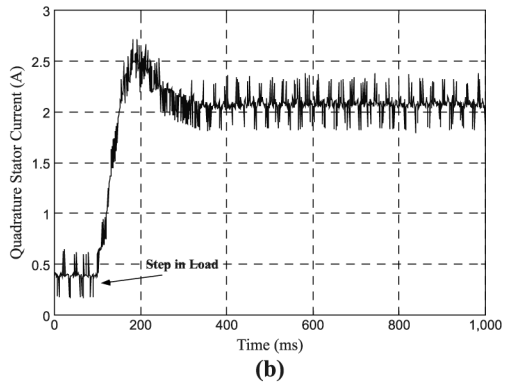

Figure 14.
Motor speed for a step change in load torque at constant reference speed of 235.6 rad/s (experimental): (a) Speed and (b) Current (i_{SQ})

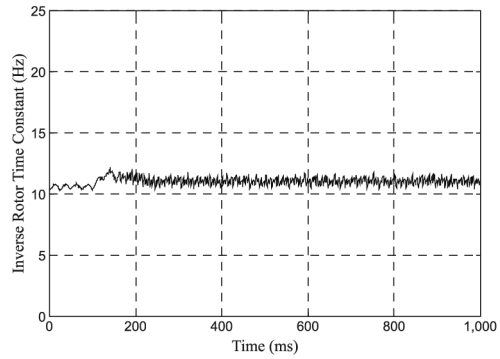

Figure 15.
Inverse rotor time constant estimation for a step in load torque at constant speed of 235.6 rad/s (experimental)

References

Ba-razzouk, A., Che′riti, A. and Rajagopalan, V. (1999), "Real time implementation of a rotor time constant online estimation scheme", *IEEE Industrial Electronics Society*, Vol. 2, pp. 927-32, 25th Annual Conference.

Benhaddadi, M., Yazid, K. and Khaldi, R. (1997), "An effective identification of rotor resistance for induction motor vector control", paper presented at the IEEE Instrumentation and Measurement Technology Conference, Ottawa, May 1997, pp. 339-42.

Choi, J.-W., Young, S.-I. and Sul, S.-K. (1996), "Inverter output synthesis using novel dead time compensation", *IEEE Transactions on Power Electronics*, Vol. 11 No. 2, pp. 221-7.

Halasz, S., Huu, B.T. and Veszpremi, K. (1995), "Rotor time constant online identification for field oriented AC drives", *Proceedings of the IEEE International Symposium on Industrial Electronics, 1995. ISIE '95*, 10-14 July, Vol. 2, pp. 654-9.

Hren, A. and Jezernik, K. (1997), "A new rotor time constant estimation method for indirect vector controlled induction motor drive", *Proceedings of the IEEE International Symposium on Industrial Electronics, ISIE'97*, 3, pp. 1029-33.

Idris, N.R.N., Yatim, A.H. and Azli, N.A. (2001), "Direct torque control of induction machines with constant switching frequency and improved stator flux", *IEEE Industrial Electronics Society*, Vol. 2, pp. 1285-91, 27th Annual Conference, IECON' 0129, November/December.

Jang, J. and Holtz, J. (1997), "High dynamic speed sensorless AC drive with on-line parameter tuning and steady state accuracy", *IEEE Transactions on Industrial Electronics*, Vol. 44 No. 2, pp. 240-6.

Krishnan, R. and Bharadwaj, A.S. (1991), "A review of parameter sensitivity and adaptation in indirect vector controlled induction motor drive systems", *IEEE Transactions on Power Electronics*, Vol. 6 No. 4, pp. 695-703.

Marwali, M.N. and Keyhani, A. (1997), "A comparative study of rotor flux based MRAS and back EMF based MRAS speed estimators for speed sensorless vector control of induction machines", *IEEE Ind. Society Annu. Meeting*, New Orleans, LA, October 1997, pp. 160-6.

Moreira, J.C., Hung, K.T., Lipo, T.A. and Lorenz, R.D. (1992), "A simple robust adaptive controller for detuning correction in field oriented induction machines", *IEEE Transactions on Industry Applications*, Vol. 28 No. 6, pp. 1359-66.

Nait Said, M.S. and Benbouzid, M.E.H. (1999), "Induction motor direct field oriented control with robust online tuning of rotor resistance", *IEEE Transactions on Energy Conversion*, Vol. 14 No. 4, pp. 1038-42.

Ouhrouche, M.A. and Volat, C. (2000), "Simulation of a direct field oriented controller for induction motor using MATLAB/SIMULINK software package", *Proceedings of the IASTED International Conference Modelling and Simulation*, (MS' 2000), Pittsburgh, PA, May, pp. 298-302.

Robyns, B., Sente, P.A., Buyse, H.A. and Labrique, F. (1999), "Influence of digital current control strategy on the sensitivity to electrical parameters uncertainties of induction motor indirect field-oriented control", *IEEE Transactions on Power Electronics*, Vol. 14 No. 4, pp. 690-9.

Schauder, C. (1992), "Adaptive speed identification for vector control of induction motors without rotational transducer", *IEEE Transactions on Industry Applications*, Vol. 28 No. 5, pp. 1054-61.

Shi, K.L., Chan, T.F. and Wong, Y.K. (1997), "Modeling of the three phase induction motor using SIMULINK", *Electric Machines and Drives Conference Record, 1997*, IEEE International, pp. WB3/6.1-WB3/6.3.

Shieh, H.J., Shyu, K.K. and Lin, F.J. (1998), "Adaptive estimation of rotor time constant for indirect field-oriented induction motor drive", *IEE Proceedings-Electric Power Applications*, Vol. 145, pp. 111-8.

Shyu, K.-K., Shieh, H.-J. and Liu, C.-C. (1996), "Adaptive field-oriented control of induction motor with rotor flux observation", *Proceedings of the IEEE International Conference on Industrial Electron., Control, and Instrum.*, IECON 22 August, Vol. 2, pp. 1204-9.

Sullivan, C.R., Kao, C., Acker, B.M. and Sanders, S.R. (1996), "Control systems for induction machines with magnetic saturation", *IEEE Transactions on Industrial Electronics*, Vol. 43 No. 1, pp. 142-52.

Toliyat, H.A., Arefeen, M.S., Rahman, K.M. and Figoli, D. (1999), "Rotor time constant updating scheme for a rotor flux-oriented induction motor drive", *IEEE Transactions on Power Electronics*, Vol. 14 No. 5, pp. 850-6.

Trzynadlowski, A.M. (1994), *The Field Orientation Principle in Control of Induction Motors*, Kluwer Academic Publishers, Norwell, MA.

Wade, S., Dunnigan, W.M. and Williams, B.W. (1997), "Modeling and simulation of induction machine vector control with rotor resistance identification", *IEEE Transactions on Power Electronics*, Vol. 12 No. 3, pp. 495-506.

Yu, X., Dunnigan, M.W. and Williams, B.W. (2000), "Phase voltage estimation of a PWM VSI and its application to vector-controlled induction machine parameter estimation", *IEEE Transactions on Industrial Electronics*, Vol. 47 No. 5, pp. 1181-5.

Appendix 1

3∅ Y-connected, squirrel-cage induction motor	3∅ Δ-connected, squirrel-cage induction motor
Rated power: 7.46 kW	Rated power: 0.37 kW
Rated stator voltage: 220 V	Rated stator voltage: 230 V
Rated frequency: 60 Hz	Rated frequency: 50 Hz
No. of poles: $P = 6$	No. of poles: $P = 2$
Stator resistance: $R_s = 0.294\,\Omega$/ph	Stator resistance: $R_s = 24.6\,\Omega$/ph
Rotor resistance: $R_r = 0.156\,\Omega$/ph	Rotor resistance: $R_r = 16.1\,\Omega$/ph
Stator inductance: $L_s = 0.0424$ H/ph	Stator inductance: $L_s = 1.49$ H/ph
Rotor inductance: $L_r = 0.0417$ H/ph	Rotor inductance: $L_r = 1.49$ H/ph
Magnetizing Inductance: 0.041 H/ph	Magnetizing Inductance: 1.46 H/ph
Mass moment of inertia: $J = 0.4\,\text{kgm}^2$	Mass moment of inertia: $J = 3.5 \times 10^{-4}\,\text{kgm}^2$

Table AI.
Motors parameters

Appendix 2. List of symbols

$*$ (superscript)	: indicates a reference quantity.
$\hat{}$	: Indicates an estimated quantity.
B	: Coefficient of viscosity.
d, q (subscript)	: stator reference frame d and q components.
D, Q (subscript)	: Synchronously rotating reference frame D and Q components.
i_r	: Rotor current vector.
i_s	: Stator current vector.
v_r	: Rotor voltage vector.
v_s	: Stator voltage vector.
$\boldsymbol{\lambda}_r$	: Rotor flux vector.
$\boldsymbol{\lambda}_s$	: Stator flux vector.
$\boldsymbol{\omega}_r$	: Electrical angular frequency of the rotor (rad/s).
$\boldsymbol{\omega}_{sl}$	: Slip angular frequency (rad/s).
$\boldsymbol{\omega}_e$	: Angular frequency of synchronously rotating reference frame $\boldsymbol{\omega} = \boldsymbol{\omega}_r + \boldsymbol{\omega}_{sl}$ (rad/s).
$\boldsymbol{\omega}_m$	: Mechanical angular frequency of the rotor (rad/s)
j	: Imaginary number $\sqrt{-1}$.
J	: Moment of inertia.
L_m	: Magnetizing inductance.
L_r	: Rotor leakage inductance.
L_s	: Stator leakage inductance.

R_s : Stator resistance.
G_r : Inverse rotor time constant ($= R_r/L_r$).
$\hat{G}_r$: : Estimated inverse rotor time constant.
G_{non} : Nominal inverse rotor time constant ($1/\tau_{r\,nom}$).
S : Differential operator d/dt.
σ : Total leakage factor ($= 1 - (L_m^2/L_sL_r)$).

Appendix 3. Root locus

Figure A1-A3

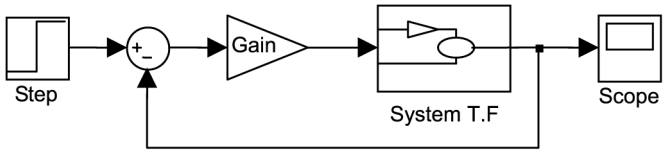

Figure A1.
Closed loop system for equation (32)

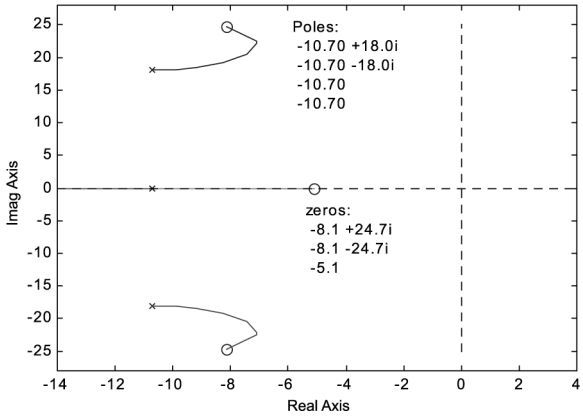

Figure A2.
Root Locus plot for nominal speed and load (0.37 kW motor)

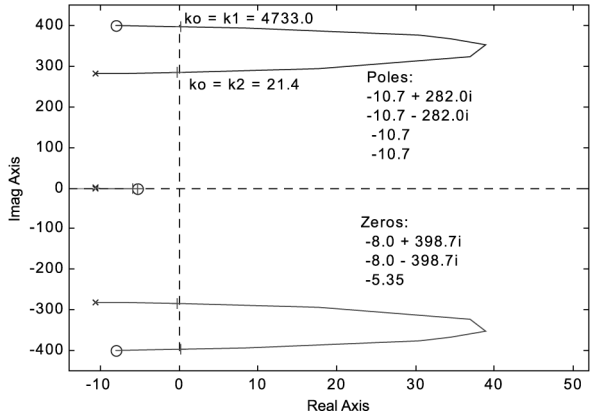

Figure A3.
Root Locus plot for low speed under no load (0.37 kW motor)